World Academy of Science, Engineering and Technology
International Journal of Biomedical and Biological Engineering
Vol:3, No:4, 2009

An Automated Method to Segment and Classify Masses in Mammograms

Viet Dzung Nguyen, Duc Thuan Nguyen, Tien Dzung Nguyen, Van Thanh Pham

***Abstract*—**Mammography is the most effective procedure for an early diagnosis of the breast cancer. Nowadays, people are trying to find a way or method to support as much as possible to the radiologists in diagnosis process. The most popular way is now being developed is using Computer-Aided Detection (CAD) system to process the digital mammograms and prompt the suspicious region to radiologist. In this paper, an automated CAD system for detection and classification of massive lesions in mammographic images is presented. The system consists of three processing steps: Regions-Of-Interest detection, feature extraction and classification. Our CAD system was evaluated on Mini-MIAS database consisting 322 digitalized mammograms. The CAD system's performance is evaluated using Receiver Operating Characteristics (ROC) and Free-response ROC (FROC) curves. The archived results are 3.47 false positives per image (FPpI) and sensitivity of 85%.

***Keywords*—**classification, computer-aided detection, feature extraction, mass detection.

I. Introduction

BREAST cancer is considered as one of the most dangerous diseases to woman [1]. It is causing death for quite large number of women among the age of 40 and above every year. According to a study of International Agency for Research on Cancer (IARC), in 1998, breast cancer is the highest rate disease in women worldwide, with the rate about 92.04 (over 100000 people) in European Union, and about 64.48 (over 100000 people) worldwide in 1998. Besides that, breast cancer is gradually becoming popular in the developing countries. In Viet Nam, there are about 20.3 people for every 100000 women having breast cancer in large cities in 1998 [2]. For that reason, breast cancer is taking more concern from the radiologists as well as the researchers all over the world than ever. As long as breast cancer is detected and treated early, women can recover health soon and reduce mortality rate. By far, mammography is widely recognized as the only imaging modality that is useful for the early detection of the abnormalities indicating the presence of a breast cancer [3]. Early detection of breast cancer is usually realized by mammographic screening programs. Screening programs are based on a double visual inspection of the mammographic images, since double reading increases the diagnostic accuracy [4]. Although mammography is seem high effective, the diagnosis is mainly based on the radiologist's experiences and some conditional factors such as stress, distraction, fatigue or low ability of eyes at that time.

Reports show that currently, the diagnosis can only achieve 75% accuracy [5] and most radiologists encourage biopsies for the final diagnosis. The causes of these false negative screening examinations are not clear. The clinical significance of the early diagnosis and the difficulty of the diagnostic task have generated a tremendous interest in developing Computer-Aided Detection (CAD) schemes [6-8] for mammographic interpretation. The computer scheme acts as a "second reader", pointing out to the radiologist, abnormalities which otherwise might have been missed. The final diagnosis is made by the radiologist [9].

Masses, as well as microcalcification clusters, are often clear marks of a breast neoplasia. While microcalcifications are small (their diameter are approximate 0.1 ÷ 1.0 mm) and brilliant objects, masses are rather large (their diameter are approximate 1.0 cm) with various shapes and show up with faint contrast. Masses are classified by their shapes and margins as shown in Fig. 1.

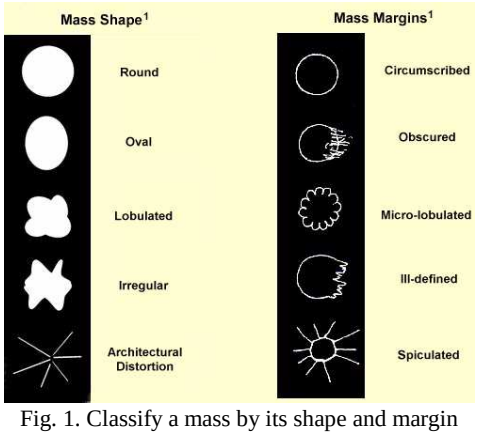

Fig. 1. Classify a mass by its shape and margin

Due to irregular shapes and ill-defined margins of mass, the identification of massive lesions requires a dedicate strategy.

This paper is part of project B2009-01-156 sponsored by Vietnamese Ministry of Education and Training

Viet Dzung Nguyen is with Biomedical Electronics Center, Hanoi University of Science and Technology, Hanoi, Vietnam (corresponding author, phone: 84-4-38682099; fax: 84-4-28682099; email: nvdung-bme@mail.hut.edu.vn).

Duc Thuan Nguyen is with Department of Biomedical Engineering, Faculty of Electronics and Telecommunications, Hanoi University of Science and Technology, Hanoi, Vietnam (e-mail: ndthuan-qlkh@mail.hut.edu.vn).

Tien Dzung Nguyen is with Department of Electronics and Computer Engineering, Faculty of Electronics and Telecommunications, Hanoi University of Science and Technology, Hanoi, Vietnam (e-mail: dungnt-fet@mail.hut.edu.vn).

Van Thanh Pham is with Comit Inc, Hanoi, Vietnam (email: pleheme@yahoo.com.vn).

In this paper, we present an automated CAD system to detect and classify massive lesions in mammograms. The system consists of 3 processing levels: Regions-Of-Interest detection or mass detection, feature extraction and classification. These levels are discussed in following sections.

II. Database

In this study, we use mammogram database Mini-MIAS to test the algorithm presented. The database MIAS is created from the Mammographic Image Analysis Society - an organization of United Kingdom research groups. This database includes 322 digital mammograms from 161 patients. Films taken from the United Kingdom National Breast Screening Program have been digitized to 50 micron pixel edge, and presenting each pixel with an 8-bit word. Every image in database always has extra-information or ground truth from the radiologists about characteristic of background tissue, type of abnormality present, severity of abnormality, the coordinates of center and approximate radius (in pixels) of a circle enclosing the abnormality.

Mini-MIAS database [10] is a kind of reduced type of database MIAS, the original MIAS database (digitized at 50 micron pixel edge) has been reduced to 200 micron pixel edge and clipped/padded so that every image has a size of 1024 x 1024 pixels.

III. Mass Detection

An important step in CAD system is the mass detection. The goal of this step is to extract from the background one or more regions of interest (ROIs) which are likely contain a mass. This is not a trivial task due to the ill-defined borders, which make difficult their discrimination from the parenchyma's structures. The accuracy of this process will affect strongly the following classification step.

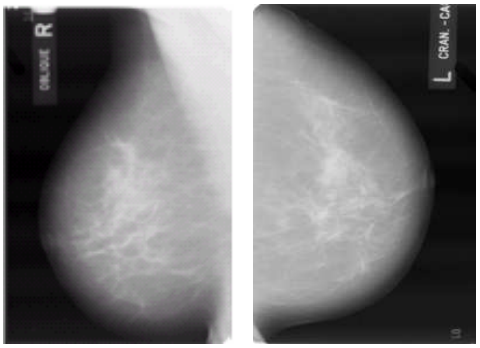

Fig. 2. Labels in mammograms

As shown in Fig. 2, image's label is usually existed. So that, in order to reduce the processing time for mass detection process as well as to increase accuracy of the process, prior to mass detecting, the image's label must be removed. It can be done as follows:

- Use a fixed global threshold to divide the image into separated regions.
- Label pixels in each region.
- Calculate the number of pixels in each region.
- Retain the biggest region, eliminate the others.

Usually, mass detection methods can be classified into four main categories: thresholding techniques, edge-based methods, region-based methods, and hybrid methods. In this paper, we proposed an edge-based mass detection algorithm. The proposed algorithm works as follows:

- Searching on whole the breast portion of the mammogram a maximum gray level I_M.
- An iso-intensity contour, including the pixel of the maximum intensity, is draw at a threshold value $I_{th} = I_M / 2$, thus delimiting a ROI with area A_R.
- A fixed threshold for comparison is defined as $I_C = 3.I_M / 4$.
- The threshold I_{th}

  + is increased by an amount which is one eighth of the previous one if the ROI area A_R is greater than a limit area A_L and $I_{th} < I_C$.

  + is increased by an amount which is one fourth of the previous one if the ROI area A_R is greater than a limit area A_L and $I_{th} \geq I_C$.
- The iteration is stopped when the ROI area A_R is smaller than the limit area A_L or the difference between two consecutive thresholds is less than I_Δ gray levels.
- The ROIs are stored for feature extraction and classification.

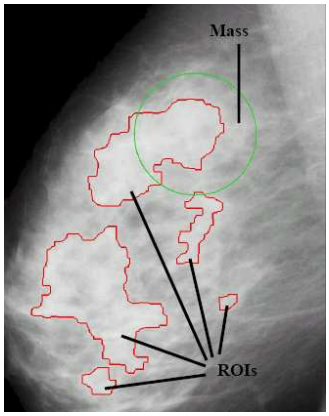

Fig. 3. Detected ROIs and confirmed mass on a mammogram

Examples of ROIs detected by the proposed mass detection algorithm are given in Fig. 3. All of detected ROIs are represented by red curves. The green circle is the circle enclosing the abnormality on the mammogram. It is drawn based on the ground truth that is come along with the mammogram. It is characterized by center coordinates (X_{rad}, Y_{rad}) and radius (R_{rad}).

Once a ROI is detected, it is labeled as true positive ROI (TP ROI) or false positive ROI (FP ROI). Draw a minimal

rectangle fully containing the ROI, with its sides are parallel with respect to the ones of the image. Assume $(2L_x, 2L_y)$ be the sizes of the rectangle and (X_{cad}, Y_{cad}) be the coordinates of the ROI. The following conditions are considered

$$\left|X_{cad} - X_{rad}\right| < max\left(R_{rad}, L_x\right) \quad (1)$$

$$\left|Y_{cad} - Y_{rad}\right| < max\left(R_{rad}, L_y\right) \quad (2)$$

The ROI is labeled as TP ROI if (1) and (2) are both satisfied. Otherwise, it is labeled as FP ROI.

The values of A_L and I_Δ were chosen as the values that maximized sensitivity of the mass detection algorithm (percentage of TP ROIs among actual masses). The best obtained values were $A_L = 192x192$ pixels and $I_\Delta = 1$ gray level. The corresponding sensitivity was 94.5% and the number of false positives per image (FPpI) was 11.3.

IV. Feature Extraction

Before going to the classification step, features of detected ROIs should be extracted or calculated. This is because the features of masses generally present distinct features from those of normal breast tissues. The extracted features are the inputs to a classifier to determine how pathological the ROI is.

Textural features have been successfully applied to detect pathologies in medical images [11-12]. In this paper we focused on calculating textural features based on Gray Level Co-occurrence Matrix (GLCM) [13]. The GLCM exploits the higher-order distribution of gray values of pixels that are defined with a specific distance or neighborhood criterion.

In the simplest form, the GLCM p_{ij} is the distribution of the number of occurrences of a pair of gray values i and j separated by a distance vector $d = (d_x, d_y)$. To achieve this matrix, we consider the minimal rectangular fully includes the ROI, specific distance $d = 1$ at quantized angles $\theta = k\pi/4$ with $k = 0,1,2,3$. Symmetry is achieved by averaging the GLCM with its transpose, thus leading to invariance under π rotations, too. Textural features can be derived from the GLCM and used in texture classification in place of the single GLCM elements. As the texture is gray tone independent, either the image must be normalized or one should choose features that are invariant under monotonic gray level transformation. At this case, we choose, among all the GLCM features, the ones that are invariant under monotonic gray tone transformation. As said above, there are four GLCM for each angles. For every GLCM three types of properties are calculated.

- Energy

$$f_1 = \sum_{ij} p_{ij}^2$$

- Entropy

$$f_2 = -\sum_{ij} p_{ij}.ln\left(p_{ij}\right)$$

- Information measures of correlation

$$f_3 = \frac{f_2 - H_1}{max\{H_x, H_y\}}$$

$$f_4 = \left[1 - exp\left\{-2\left(H_2 - f_2\right)\right\}\right]^{1/2}$$

where

$$P_x(i) = \sum_j p_{ij}$$

$$P_y(j) = \sum_i p_{ij}$$

$$H_1 = -\sum_{ij} p_{ij}.ln\left\{P_x(i).P_y(j)\right\}$$

$$H_2 = -\sum_{ij} P_x(i).P_y(j).ln\left\{P_x(i).P_y(j)\right\}$$

$$H_x = -\sum_i P_x(i).ln\left\{P_x(i)\right\}$$

$$H_y = -\sum_j P_y(j).ln\left\{P_y(j)\right\}$$

From three types of properties, average value, range and variance are computed for each $\theta = k\pi/4$, therefore there are total 12 textural features.

V. Classification

The extracted features were inputs into a classifier to determine whether the ROIs should be concerned. A number of classifiers based on linear discriminant analysis [14-15], artificial neural networks [16-18] and rule-based methods [19-20] have shown effectiveness in detection and diagnostic systems. In this study, artificial neural network is employed as the classifier. At this step, we used a supervised two-layer feed-forward neural network trained with the gradient descent learning rule for the ROI pattern classification

$$\Delta w_{ij}(\tau) = -\eta \frac{\partial E(\tau)}{\partial w_{ij}} + \alpha \Delta w_{ij}(\tau - 1)$$

$$E(\tau) = \frac{1}{2}\sum_{\mu}\left(t^{\mu} - y^{\mu}\right)^2$$

where the $E(\tau)$ function measures the error of the network outputs y^{μ} in reproducing the targets $t^{\mu} = 1,0$ at iteration τ, and w_{ij} are the network weights. The term $\alpha \Delta w_{ij}(\tau - 1)$, known as momentum, represents a sort of inertia which is added to quickly move along the direction of decreasing gradient, thus reducing the computational time to the solution. Different values of the momentum parameter α was tested and the best trade-off between performance and computational time was reached for $\alpha = 0.1 \div 0.2$. The learning rate was $\eta = 0.01$. A sigmoid transfer function is used

$$g(x) = \frac{1}{1 + e^{-\beta x}}$$

with gain factor $\beta = 1$

The number of input neurons must be equal to the number of features extracted of each ROI so the neural network consisted of $N_i = 12$ input neurons. The network classifies a

ROI into mass or healthy one hence there is only one output neuron. The neural output provides a continuos value $0 \le p \le 1$ which is used as a threshold to discriminate between mass regions and healthy ones. For each threshold value, the sensitivity and the specificity are computed.

The size of the hidden layer N_h was tuned in the range $[N_i - 1, 2N_i - 1]$ to optimize the classification performance. ROI's feature database was created. This database was divided into 2 parts. One part was for training phase and the other was for testing phase.

VI. Results

Fig. 4 depicts some results of label removal process. On the left are original images and on the right are label-removed images. The results were good. Most of labels appeared in Mini-MIAS digitalized mammograms were removed accurately. Only a small part of labels overlapped the breast portion of the mammogram could not be removed. It can be seen that not only the labels but also other artifacts in the mammogram were removed is also noted that too.

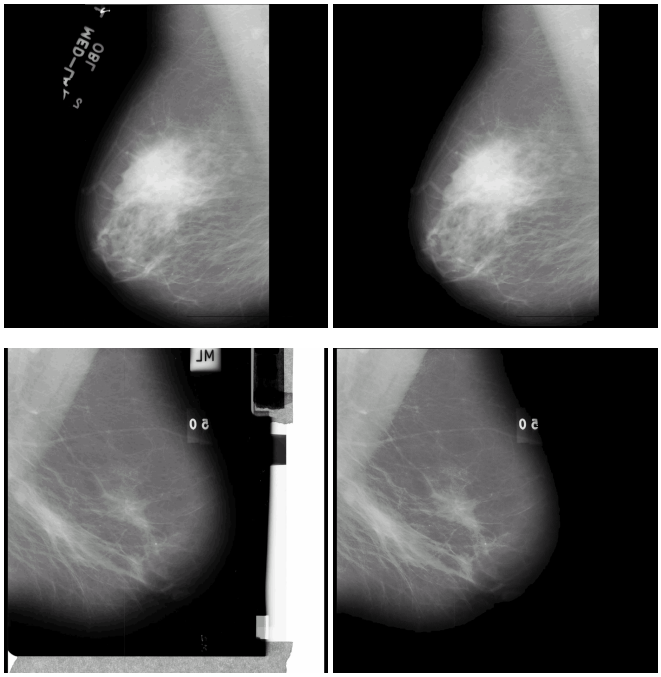

Fig. 4. Original images (left). Label-removed images (right).

As mentioned in section III, the values of A_L and I_Δ were determined in order to maximize the sensitivity of the mass detection algorithm. The best value was 94.5% with FPpI of 11.3. The mass detection result is given in Fig. 5.

To evaluate the performance of a CAD system, a Receiver Operating Characteristics (ROC) and Free-response ROC (FROC) curves are used. A ROC curve is a plotting of true positive as a function of false positive at different values of the decision threshold on the neural network output. Higher ROC, approaching the perfection at the upper left hand corner, would indicate greater discrimination capacity. While the ROC curve displays the neural network performance in classifying the ROI patterns, the free-response ROC (FROC) curve provides the performance of the overall computer aided diagnosis system in detecting the masses, as it reports the mass sensitivity against the FPpI.

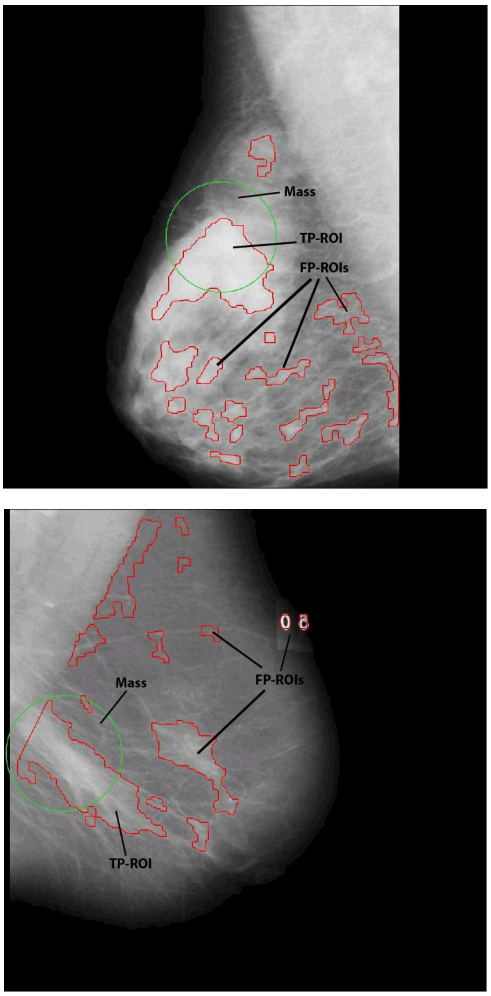

Fig. 5. ROI detection results

The ROC curve is shown in Fig. 6. The classification performance is quantified by the area A_z under the curve (AUC). The obtained AUC value $A_z = 0.815$ lies in the range $0.7 < AUC < 0.9$ therefore the classifier can be considered accurate enough [21].

FROC curve can be seen at Fig. 7, which represents the mass sensitivity of the overall system against the number of false positives per image (FPpI): 85% of mass sensitivity is achieved with 3.47 FPpI (with the efficiency of ROI hunting is 94.5%).

We also changed number of hidden nodes of the neural network and tested the number of false positives per image while the performance of overall CAD system was fixed at 85%. The result is given in table I.

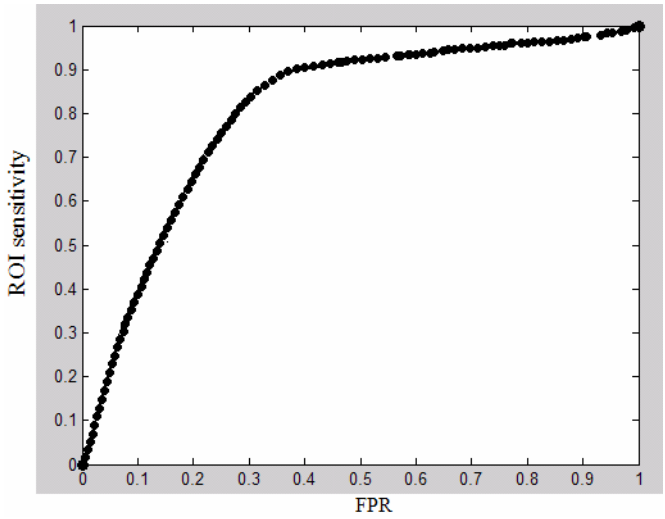

Fig. 6. ROC curve

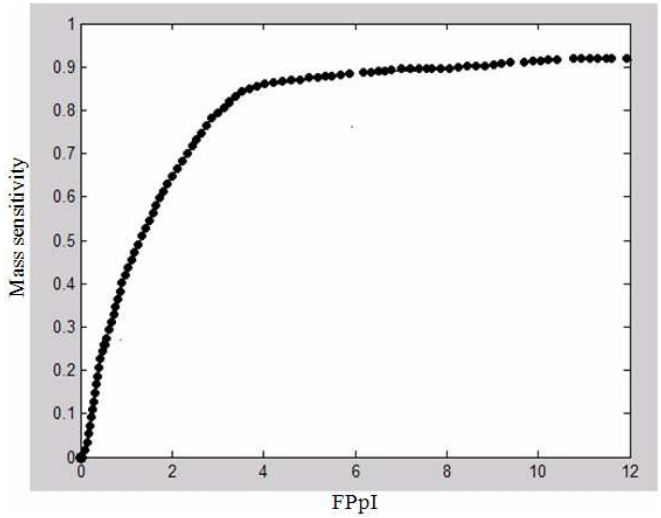

Fig. 7. FROC curve.

TABLE I
THE CAD SYSTEM PERFORMANCES

N_h	12	16	20	22	24
FPpI	10.72	3.54	3.54	3.5	3.47

VII. CONCLUSION

In this paper, an algorithm for automotive massive lesion detection has been proposed. This algorithm relied on an edge-based threshold strategy for the mass segmentation. There total 12 selected ROIs features were extracted to discriminate between two classes – mass regions and healthy ones. The discrimination performance of the algorithm has been checked by means of a supervised neural network. The results have been evaluated in terms of ROC and FROC curves. The area under the ROC curve A_z is comparable with the ones obtained in [22-23].

In future, different textural feature sets and different feature selection methods will be used also in order to improve the performance of ROI classification. Classification performance of several classifiers will also be compared to find out the optimum correct classification rate.

REFERENCES

[1] R. A. Smith, "Epidemiology of breast cancer" in *A categorical course in physics. Imaging considerations and medical physics responsibilities*, Madison, Wisconsin, Medical Physics Publishing, 1991.
[2] http://bachmai.gov.vn/index.php?option=com_content&task=view&id=771&Itemid=34
[3] A. G. Haus, M. Yaffe (editors), "A categorical course in physics. Technical aspects in breast imaging", presented at 79th Scientific Assembly and Annual Meeting of Radiological Society of North America, 1993.
[4] N. Karssemeijer, J. D. Otten, A. L. Verbeek, J. H. Groenewoud, H. J. de Koning, J. H. Hendriks, and R. Holland, "Computer-aided detection versus independent double reading of masses in mammograms," *Radiology*, vol. 227, pp. 192–200, 2003.
[5] W. A. Murph, J. M. Destouet Jr, and B. S. Monsees, "Professional quality assurance for mammography screening programs," *Radiology*, vol. 175, pp. 319-320, 1990.
[6] C. J. Viborny, "Can computer help radiologists read mammograms?," *Radiology*, vol. 191, pp. 315-317, 1994.
[7] C. J. Viborny, M. L. Giger, and R. M. Nishikawa, "Computer aided detection and diagnosis of breast cancer," *Radiologic Clinics of North America*, vol. 38(4), pp. 725-740, 2000.
[8] G.D. Tourassi, R. V. Voracek, "Computer-assisted detection of mammographic masses: a template matching scheme based on mutual information", Medical. Physics, vol. 30, pp. 2123–2130, 2003.
[9] U.Bick and K. Doi, Computer Aided Diagnosis Tutorial, CARS 2000 "Tutorial on Computer Aided-Diagnosis". Hyatt Regency: San Francisco, USA, 2000.
[10] http://peipa.essex.ac.uk/info/mias.html
[11] N. R. Mudigonda, R. M. Rangayyan, and J. E. Leo Desautels, "Gradient and texture analysis for the classifcation of mammographic masses," *IEEE Transactions on Medical Imaging*, vol. 19(10), pp. 11032-1043, 2000.
[12] K. Bovis, S. Singh, "Detection of masses in mammograms using texture features," in *Proceeding of 15th International Conference on Pattern Recognition*, pp. 267-70, 2000.
[13] R. M. Haralik, K. Shanmugam, and I. Dinstein, "Textural features for image classification," *IEEE Trans. Syst. Man Cyber*, SMC-3, pp. 610–621, 1973.
[14] H. P. Chan, D. Wei, M. A. Helvie, B. Sahiner, D. D. Adler, M. M. Goodsitt, and N. Petrick, "Computer-aided classification of mammographic masses and normal tissue: linear discriminant analysis in texture feature space," *Physics in Medicine and Biology.*, vol. 40, pp. 857–876, 1995.
[15] H. P. Chan, B. Sahiner, M. A. Helvie, N. Petrick, M. A. Roubidoux, T. E. Wilson, D. D. Adler, C. Paramagul, J. S. Newman, and S. Sanjay-Gopal, "Improvement of radiologists' characterization of mammographic masses by using computer-aided diagnosis: an ROC study," *Radiology*, vol. 212, pp. 817–827, 1999.
[16] G. te Brake and N. Karssemeijer, "Segmentation of suspicious densities in digital mammograms," *Medical Physics*, vol.28, pp. 259-266, 2001.
[17] Y. Wu, M. L. Giger, K. Doi, C. J. Vyborny, R. A. Schmidt, and C. E. Metz, "Artificial neural networks in mammography: Application to decision making in diagnosis of breast cancer," *Radiology*, vol. 187, pp. 81-87, 1993.
[18] B. Zeng, Y. Chang, W. F. Good, and D. Gur, "Performance gain in computer-assisted detection schemes by averaging scores generated from artificial neural networks with adaptive filtering," *Medical Physics*, vol. 28, pp. 2302-2308, 2001.
[19] H. P. Chan, D. Wei, M. A. Helvie, B. Sahiner, D. D. Adler, M. M. Goodsitt, and N. Petrick, "Computer-aided classification of mammographic masses and normal tissue: linear discriminant analysis in texture feature space," *Physics in Medicine and Biology.*, vol. 40, pp. 857–876, 1995.

[20] H. P. Chan, B. Sahiner, M. A. Helvie, N. Petrick, M. A. Roubidoux, T. E. Wilson, D. D. Adler, C. Paramagul, J. S. Newman, and S. Sanjay-Gopal, "Improvement of radiologists' characterization of mammographic masses by using computer-aided diagnosis: an ROC study," *Radiology*, vol. 212, pp. 817–827, 1999.
[21] J. A. Swets, "Measuring the accuracy of diagnostic systems," *Science*, vol 240, pp. 1285–1293, 1988.
[22] B. Sahiner, N. Petrick, H.P. Chan, L.M. Hadjiiski, C. Paramagul, M.A. Helvie, M.N. Gurcan, "Computer-Aided characterization of mammographic masses: accuracy of mass segmentation and its effects on characterization," *IEEE Transaction on Medical Imaging*, vol. 20, no. 12, pp. 1275-1284, 2001.
[23] D.M. Catarious Jr., A.H. Baydush, C.E. Floyd Jr, "Incorporation of an iterative, linear segmentation routine into a mammographic mass CAD system," *Medical Physics*, vol. 31, pp. 1512-1520, 2004.